Environmental Science and Pollution Research (2024) 31:34309–34323
https://doi.org/10.1007/s11356-024-33521-5

RESEARCH ARTICLE

Non-conservative behavior of organic matter and its interaction with metals in an equatorial estuary, Brazil

Mariany Sousa Cavalcante[1] · **Rozane Valente Marins**[1] · **Stéphane Mounier**[2]

Received: 16 October 2023 / Accepted: 27 April 2024 / Published online: 3 May 2024

Abstract

Droughts are becoming more intense and frequent in the Brazilian semiarid because of El Niño and global climate changes. The Jaguaribe River estuary is a semiarid ecosystem that experiences a reduction in freshwater discharges due to droughts and river damming. The decrease in freshwater fluxes has increased metal availability through the water residence time increase in the Jaguaribe River estuary. Then, this study aimed to evaluate the dissolved organic matter quality and its interaction with metals in the Jaguaribe River estuary after a severe drought period. It was performed through carbon analyses, fluorescence spectroscopy, ultrafiltration technique, and determinations of metals by ICP-MS. Optical analysis showed that the dissolved organic carbon (DOC) was preponderantly composed of terrestrial-derived humic compounds, while the low ratio between the particulate organic carbon (POC) and chlorophyll-a indicated that POC was predominantly phytoplankton-derived. DOC and POC presented non-conservative removal during the estuarine mixing. DOM and dissolved elements were mostly distributed within the LMW fraction and presented a low percentage in the colloidal fraction. Li, Rb, Sr, Mo, and U showed conservative behavior, while Cu, Fe, Cr, and V had non-conservative behavior with a significant positive correlation with DOM, suggesting DOM as a relevant driver of metal availability at the Jaguaribe River estuary even during the rainy season.

Keywords PARAFAC · Partitioning · Aromaticity · Ultrafiltration · Fluorophores

Introduction

Trace metals contamination is a serious concern in the aquatic systems because they are major environmental contaminants and have long-term accumulation in sediments and organisms. Their speciation and consequently fate, transport, bioavailability, and toxicity in estuaries is tightly related to organic matter dynamic (Simpson et al. 2014) and environmental conditions (pH, ionic strength, and competition with other cations) (Louis et al. 2009). Due to organic matter role in binding and stabilizing metals and contaminants in estuaries (Wang et al. 2017), efforts to access information about the composition and partitioning of organic matter, in the dissolved, colloidal, and particulate phases, have increased over the last years (Stolpe et al. 2010, 2014; Zhou and Guo 2015; Yan et al. 2021).

The dissolved organic matter (DOM) is a heterogeneous mixture of molecules derived from the biological decomposition and metabolic activity of organisms (Findlay and Sinsabaugh 2003), presenting different sizes under 0.22 µm, functionalities, ages, and origins (allochthonous and autochthonous). DOM is ubiquitous in marine environments and plays important role in biogeochemical and environmental processes, such as the carbon and nutrients cycling, energy source to consumers, and water quality (Wang et al. 2007; Santinelli et al. 2010; Yang et al. 2016). The isolation and separation of aquatic colloids are typically preceded by the filtration of samples through 1–0.2 µm pore-size filters (Wilkinson and Lead 2007). Crossflow ultrafiltration has been widely used to fractionate DOM into different size and molecular weight fractions (Wilkinson and Lead

Responsible Editor: V.V.S.S. Sarma

✉ Mariany Sousa Cavalcante
cavalcante.mariany@gmail.com

Rozane Valente Marins
rmarins@ufc.br

Stéphane Mounier
stephane.mounier@univ-tln.fr

[1] Instituto de Ciências do Mar, Universidade Federal do Ceará, Avenida Abolição, Fortaleza, Ceará 60165-081, Brazil

[2] Mediterranean Institute of Oceanography, Université de Toulon, Av. de L'Université, 83130 Toulon, France

2007; Wang et al. 2017; Xu and Guo 2017), such as reverse osmosis (Louis et al. 2009) and flow field–flow fractionation (Stolpe et al. 2014).

The high molecular weight (HMW) fraction is usually referred to as colloidal organic matter (COM) and is defined as macromolecules or aggregates that have size between 1 nm to 1 µm, while the low molecular weight (LMW) corresponds to molecules smaller than 1 kDa (Wilkinson and Lead 2007) and named truly dissolved organic matter (TDOM). COM is very reactive due to its high specific surface area and abundance of complexing sites that can contribute to the metal binding (Fang et al. 2015; Louis et al. 2009). In estuarine waters, metals such as copper (Cu), iron (Fe), mercury (Hg), and zinc (Zn) are found primarily in the colloidal form (Simpson et al. 2014; Luan and Vadas 2015; Wang et al. 2017). However, DOM in estuarine waters can suffer partitioning changes between the dissolved and particulate phases, through mixing processes such as flocculation, aggregation, and disaggregation (Giani et al. 2005; Yi et al. 2014; Xu et al. 2018) and alter the metals' behavior.

The characterization of DOM allows the estimation of the complexation capacity of metals by this geochemical support and thus to improve the understanding of the role of OM on the metal cycle and availability. Fluorescence spectroscopy has been widely used to characterize the nature of the part of the chromophoric dissolved organic matter (CDOM), the component of DOM that absorbs light over a wide range of ultraviolet and visible wavelength, by measuring the fluorescent dissolved organic matter (FDOM). This technique is highly sensitive, selective, easy to use, and needs small samples (Coble 2007; Fellman et al. 2009). The detailed mapping of the FDOM properties produces excitation-emission matrices (EEM) built by the merging excitation and emission wavelength domains, which are suitable for multivariate data analysis techniques such as PARAFAC ("Parallel Factor Analysis") (Wang et al. 2015; Lin et al. 2016; Shin et al. 2016; Xu and Guo 2017). Through the decomposition of a set of EEMs, the PARAFAC analysis quantifies the significant number of independent fluorescent components.

The Jaguaribe River is the major watershed in Ceará State (NE Brazil), responsible for ensuring human water supply to Fortaleza City (around 3.6 million inhabitants) and other smaller cities. However, it is under a semiarid climate in the region called "Drought Polygon" that suffers from severe droughts caused by the El Niño phenomenon and global climate changes (Marengo et al. 2020; Soares et al. 2021). As water is a scarce resource, several dams were constructed along the river to improve water availability and regulate its flow (Campos et al., 2000). Then, drought and river damming have reduced freshwater discharge to the estuary, causing modifications in the ecosystem such as intensification of hypersalinity conditions (Soares et al. 2021), mangrove expansion (Lacerda et al. 2020), and possibly decrease of OM concentrations and fluxes (Cavalcante et al. 2021). In such a scenario, the sources (marine vs. terrestrial) and quality of the OM can change. All this alters not only OM reactivity but also the estuary functioning due to its key role in the biogeochemical process as bacterial production, trophic web organization, metal complexation, and carbon cycling (Shin et al. 2016; Vazquez et al. 2011).

Despite the Jaguaribe River estuary being located in the rural area, mercury (Hg) concentrations in oysters and sediments increased surprisingly within the past 13 years due to the remobilization from soils and sediments caused by regional environmental changes (Costa and Lacerda 2014; Rios et al. 2016), showing levels as high as some metropolitan sites. Besides, Moura and Lacerda (2018) observed that Hg concentrations in tissues of organisms from the estuary marine-influenced portion were higher than those from the fluvial portion, pointing to the importance of hydrodynamic variables in controlling the hydrochemistry and Hg bioavailability (Lacerda et al. 2013, 2020).

Since OM is probably an essential parameter to the biota contamination by metals in the Jaguaribe River estuary, this study determined the UV–visible absorption spectra, EEMs fluorescence, dissolved and particulate organic carbon (DOC, POC) concentrations, dissolved metals (Al, Fe, Cu, Ni, Pb, Cr, V, Sn, Sr, Rb, Li, Mo, U) concentrations and hydrochemical parameters of water to (1) access the quality, sources, and mixing behavior of DOM and (2) evaluate the interaction between DOM and metals in the Jaguaribe River estuary. Aluminum (Al), Fe, Cu, lead (Pb), nickel (Ni), chromium (Cr), stannium (Sn), and vanadium (V) were chosen because they are toxic (except Fe) and their behavior is influenced by OM (Tribovillard et al. 2006; Gustafsson 2019). The other metals were chosen to evaluate sampling and analysis quality since they have conservative behavior.

Materials and methods

Study location and sampling strategy

The Jaguaribe River estuary is located within the Northeastern coast of Brazil (Fig. 1), presenting an annual rainfall rate of 913 mm during the past 30 years (FUNCEME, 2017). However, the Brazilian semiarid climate has a strong seasonal rainfall regime intensified by global climate change. The sampling campaign occurred in April 2018, during the rainy season, after years of severe drought that lasted from 2012 to 2017 (Marengo et al. 2017, 2020). The period between 2015 and 2016 was the peak of the drought due to the effect of the El Nino event (Dantas et al. 2020). In 2018, the annual rainfall was 1131 mm and the composed

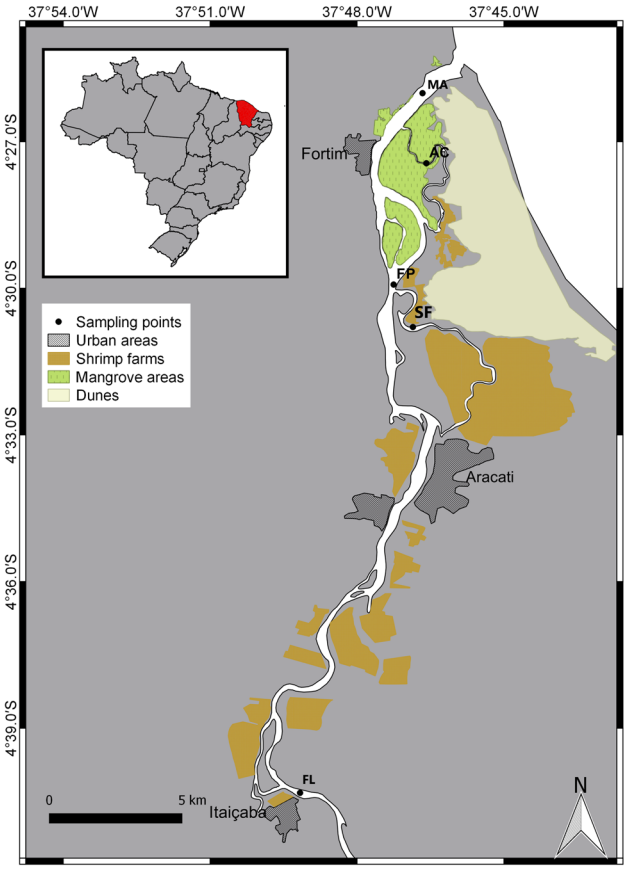

Fig. 1 Study area and sampling stations

precipitation 15 days before the campaign was 294 mm (50 mm above normal for the month).

Aquaculture, urban, and rural activities are significant sources of nutrients and probably organic matter (Eschrique et al. 2010) to the Jaguaribe River estuary. Emission factors of nitrogen and phosphorus point out that anthropogenic sources surpass the natural sources in at least one order of magnitude (Lacerda et al. 2008). Aquaculture is the most relevant source of nutrients to the estuary, followed by wastewater and husbandry. Shrimp farming presents high emission factors for Cu and Hg per unit area. Although the annual discharge of shrimp farm is smaller than the other sources (Lacerda et al. 2006, 2011), it presents high emission factors for Cu and Hg per unit area. Besides, the untreated effluents are disposed directly into estuarine waters, and most of Hg is found as dissolved species (Costa et al. 2013).

The tidal regime is semidiurnal and meso-tide, with maximum amplitude reaching 3.0 m (Dias et al. 2011). Freshwater discharges dropped from 60/130 m^3s^{-1} to 20 m^3s^{-1} after the built of major dams of the Jaguaribe River (Dias et al. 2013). As a consequence of the low freshwater supply, the tidal intrusion landward in the Jaguaribe River estuary (Dias et al. 2016) has caused several impacts as the retention of contaminants (Lacerda et al. 2020), mangrove expansion (Godoy and Lacerda 2014, 2015), reduction of sediment (Dias et al. 2013, 2016), and organic matter (Cavalcante et al. 2021) from watershed to estuary, causing high saline conditions (Marins et al. 2003; Dias et al. 2016).

Five sampling stations were distributed in the estuary (Fig. 1) to collect the water samples and to measure the hydrochemical parameters. A temporal sampling was performed to evaluate the tidal influence in the organic matter quality and its interaction with trace metals in a fixed point at the middle estuary. Every hour and a half, for 9 h (from 8 am to 5 pm), water samples were taken in the fixed point, similarly to a previous evaluation of the dynamics and sources of carbon in the estuarine maximum turbidity zone of the Jaguaribe River (Mounier et al. 2018; Cavalcante et al. 2021). These samples were numbered from 1 to 7, following the temporal order of sampling. This strategy was used to allow monitoring the changes in OM characteristics over the years with the increase of human pressure and climate changes in the region. Cavalcante et al. (2021) observed a reduction greater than 50% in the OM concentrations, compared to Mounier et al. (2018) study developed in 2004, probably due to the decrease in annual rainfall and river damming.

The fluvial end-member (salinity < 0.5) was sampled downstream the Itaiçaba dike (FL station), and the marine endmember (MA) at the estuarine mouth. Besides, samples from the Cumbe cannel (SF) and Amor Creek (AC) were taken. The Cumbe Creek is heavily impacted by shrimp farm activity since they discharge their effluents directly into it (Costa et al. 2013). Differently, the Amor creek is surrounded by a well-preserved mangrove area.

A portable YSI multiparametric probe (model professional plus) was used to measure salinity, temperature and dissolved oxygen, and a portable pH meter (Metrohm) to pH. Subsurface water (0.5 m) was sampled with an acrylic Van Dorn bottle, totaling 11 samples. Immediately after sampling, water samples were filtered through pre-combusted (at 450 °C, 12 h) and acid-washed glass microfiber filters Whatman with a 0.7 µm mesh to collect suspended particles for further analysis of particulate organic carbon and particulate nitrogen (POC, PN) and suspended particulate material (SPM). After filtration, 200 mL samples were conserved by the addition of sodium azide (NaN_3) (1 mM final concentration, so typically 200 µL of 1 M NaN_3 in 200 mL) in the fridge, avoiding biological development and further OM alteration until posterior chemical analyses in the laboratory. Chlorophyll *a* (Chl-*a*) was quantified in samples retained in AP40 fiberglass filters until saturation.

The tidal curve was plotted based on data provided by Diretoria de Hidrografia e Navegação do Brasil for the Areia Branca—Termisa (RN) port. They corresponded to three values of water level for the day of sampling (two at high

tide and one at low tide), considering the 3-h delay of the gravity wave between the Areia Branca—Termisa (RN) port and the interior of the Jaguaribe estuary calculated by Dias (2007).

ICP-MS analyses

Li, Rb, Sr, Mo, U, Sn, Pb, Cu, Ni, Fe, Al, V, and Cr concentrations in the bulk samples were determined by inductively coupled plasma mass spectrometry (ICP-MS, Laboratory MIO-Marseille). Samples were diluted (2 times) with acidified Milli-Q water to avoid the effect of salt concentrations. Indium (In) was used as an internal standard for quality control.

Crossflow ultrafiltration treatment

Three extra subsurface water samples (20 L each one) were pumped from the fixed point during the high (8 am), the slack (9:30 am), and low (11 am) tide that corresponded to points 1, 3, and 5 with a salinity of 14.8, 6.8, and 3.4, respectively. A pre-filtration of samples was done with a 0.7 µm filter to obtain the bulk samples. After, DOM fractionation between colloidal and truly dissolved phases was performed by ultrafiltration method, using sequential and tangential flow filtration system (Pellicon 2—Millipore). The cartridges used had a porosity of 0.1 µm, 10 kDa, and 1 kDa molecular weight cut-off. Metals in colloidal and truly dissolved phases were measured in the samples 3 and 5.

The material retained in these cartridges was concentrated to a volume of approximately 200 mL, resulting in three fractions to each sample (> 0.1 µm, > 10 kDa, and > 1 kDa). At the end of the experiment, seven sub-samples were obtained from each sample: one bulk, three concentrated, and three permeate samples. The concentration factor of the ultrafiltration (Fc) is the ratio between the volumes of permeate (Vp) and retentate (Vr) fractions to each membrane (Online Resource 1). Permeate solutions were saved (200 mL) to verify the efficiency of the ultrafiltration system by a mass balance of DOC and metals. The recoveries (%) in the ultrafiltration process can be calculated as follows:

$$R(\%) = \left[(Cp \times Vp) + (Cr \times Vr)\right] / [Cb \times Vb] \times 100$$

where Cb, Cp, and Cr represent DOC and metals concentrations in the bulk, permeate, and retentate, respectively, just like Vb, Vp, and Vr correspond to the volume of the bulk (Vb = Vp + Vr), permeate, and retentate samples.

Before the ultrafiltration of each sample, the cartridges were washed with H_3PO_4 (0.1N) solution and 30 L of Milli-Q water to remove possible traces of samples and to neutralize the pH of the cartridges. In the concentration step of the fractions, ultrapure water was added continuously until the conductivity was below 100 µS. cm^{-1}, for the removal of excess salts that could harm the further analyses.

Measurements of Chl-a, organic carbon, and optical properties

Chlorophyll *a* (Chl-*a*) and pheophytin were quantified in samples retained in AP40 fiberglass filters until saturation, extracted in acetone, and quantified using a spectrophotometer, according to ISO 10260 (1992) protocol.

DOC was measured using oxidation in a catalytic Pt bed at 650 °C with an automated TOC analyzer (Shimadzu TOC 5000). For DOC determination, samples were earlier acidified with HNO_3 (10%) and purged with an inert gas (O_2) to remove inorganic carbon. Next, the organic carbon remaining in the acidified sample was processed. The oxidation product of DOC (CO_2) was carried by ultrapure O_2 gas to the non-dispersive infrared analysis detector (NDIR) and then quantified. The accuracy of the analysis was 98% using potassium phthalate calibration. DOC data reported the mean of three replicate injections, for which the coefficient of variance was < 2%.

Prior to elemental organic carbon and nitrogen analysis in the particulate material, the filters were treated in silver boats with HCl vapor to remove carbonates. POC and PN analyses were made using a Flash 2000 elemental analyzer (Thermo Scientific IRMS). The analytical control was performed using the certified soil reference material (Thermo Scientific, Germany), resulting in above 94% precision.

The UV absorption spectra were measured from 240 to 800 nm at medium speed on a double beam UV-1800 (Shimadzu) in 1 cm quartz. Milli-Q water was used as a reference. The absorption coefficient of CDOM, a_{254}, was calculated as a $(\lambda) = 2.303\ A\ (\lambda)\ /\ L$, where A is the absorbance, λ is the wavelength at 254 nm, and L is the cell length in meters. The specific ultraviolet absorbance (SUVA) is the aromaticity index of OM, used as a proxy for DOM reactivity and composition. SUVA is defined as the ratio between UV absorbance at $\lambda = 254$ nm with a 10 mm optical pathway and DOC concentration (mg L^{-1}) (Weishaar et al. 2003). The spectral slope ratio (S_R) was used as an indirect measure of the average molecular weight (MW), source, and exposure to photochemical degradation of CDOM in natural waters (Helms et al., 2008). S_R was calculated using a nonlinear regression technique for a shorter wavelength region (275–295 nm) and a longer wavelength region (350–400 nm) (Stedmon et al. 2000).

Fluorescence spectra of DOM samples were acquired on a HITACHI F 4500 spectrofluorometer (Triad Scientific) for spatial and temporal filtered samples. Fluorescence excitation–emission matrices (EEM) were constructed by

scanning the excitation wavelengths from 250 to 500 nm and emission wavelengths from 250 to 700 nm, both at 5-nm intervals and a scanning speed of 240 nm min^{-1}. Rayleigh and Raman's physical diffusions of light were numerically removed by the method proposed by Zepp et al. (2004). The EEMs were modeled with PARAFAC using the software progMEEF version 1.3 Graphical User Interface developed by R. Redon (http://woms18.univ-tln.fr/progmeef/). Split-half validation and residual variance core consistency diagnostic (CONCORDIA) were used to determine the number of components before the EEMs decomposition into individual components by PARAFAC analysis. The contribution of each component was represented by the maximum fluorescence Fmax (RU, Raman units) (Stedmon and Markager 2005).

Two fluorescence indices were used to characterize the DOM: the biological index (BIX) and the fluorescence index (FI). The fluorescence index (FI) was calculated as the ratio of the fluorescence intensities at emission 470 and 520 nm, respectively (excitation = 370 nm) (Cory and McKnight 2005). The BIX was the ratio of the emission wavelength of 380 nm maximum emission intensity between 420 and 435 nm, at an excitation of 310 nm.

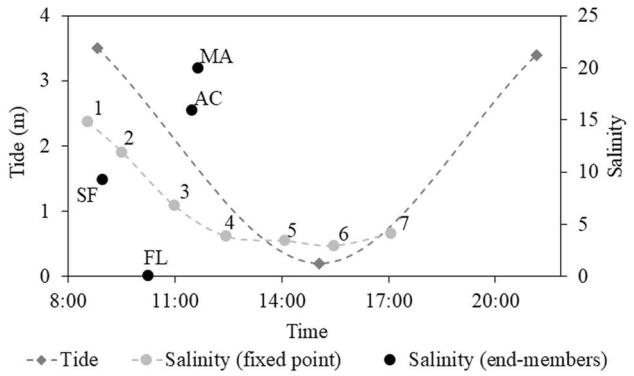

Fig. 2 Tidal and salinity variation in the Jaguaribe River estuary. Numbers and letters refer to the samples from temporal and spatial sampling, respectively

Results

Tidal, hydrochemical characteristics, and Chl-a variation in the Jaguaribe River estuary

Salinity ranged from 0.1 to 19.9, with the lowest value at the fluvial and the highest at the marine end-members, respectively. In the FP station, salinity varied from 2.9 to 14.8, reflecting the tidal variation during the temporal sampling (Fig. 2). The tide presented minimum and maximum peaks of 0.2 and 3.5 m, respectively. The spatial sampling was performed in the ebb tide, as most of the temporal sampling, to characterize the influence of continental contributions to the estuary in the rainy season but during a severe drought period in NE, BR (Marengo et al. 2020).

The pH varied from 6.80 to 7.45, with the lowest value at the fluvial end-member, increasing from upstream to downstream. At the fixed point, pH ranged from 7.01 to 7.23. The dissolved oxygen varied from 2.8 to 7.0 mg L^{-1}, with an average of 3.8 mg L^{-1}. The temporal variation was 2.8 to 3.3 mg L^{-1}, increasing linearly with pH ($R^2 = 0.83$). Chl-*a* concentrations varied between 3.2 and 25.0 µg L^{-1}, on average 13.1 ± 6.4 µg L^{-1}. The lowest Chl-*a* value corresponded to the AC station and the highest to the shrimp farm end member.

Variations of POC, DOC, CDOM, $SUVA_{254}$, and FDOM in the Jaguaribe River estuary

POC concentrations were between 65.0 and 289.9 µmol L^{-1}, with an average of 180.4 ± 88.5 µmol L^{-1}. DOC concentrations in bulk samples varied from 430.9 to 990.0 µmol L^{-1}, on average 597.0 ± 149.1 µmol L^{-1}. The theoretical conservative mixing lines were plotted using the respective DOC and POC concentrations measured in the marine and riverine end-members. POC showed an increase from salinity 0 to 5 and depletion after (Fig. 3a). DOC concentrations presented a non-conservative decrease with the salinity gradient (Fig. 3b). DOC sink from the column water occurred between the salinity 0 and 7.

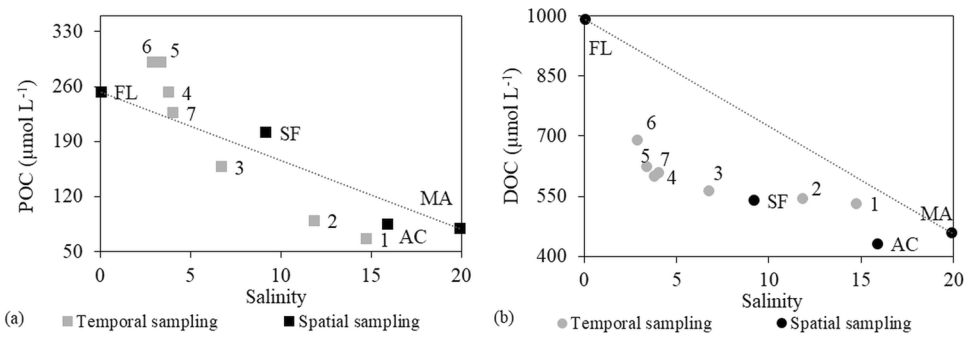

Fig. 3 Concentrations of **a** POC and **b** DOC plotted against salinity with conservative mixing line calculated from fluvial and marine end-members. Numbers and letters refer to the samples from temporal and spatial sampling, respectively

CDOM (a_{254}) varied from 40.1 to 132.9 (m^{-1}), with an average of 56.5 ± 26.4 (m^{-1}), and $SUVA_{254}$ ranged from 2.7 to 4.9 m^{-1}/(mg-C/L), with an average of 3.3 ± 0.6 m^{-1}/(mg-C/L), in the Jaguaribe River estuary. CDOM and $SUVA_{254}$ decreased with salinity non-conservatively during the temporal sampling (Fig. 4a and b). FI and BIX values respectively range from 1.23 to 1.37 (1.31 ± 0.04) and 0.43 to 0.62 (0.54 ± 0.05) in the Jaguaribe River estuary. FI and BIX decreased non-conservatively with salinity (Fig. 4c and d). S_R ranged from 1.0 to 2.2, with an average of 1.4 ± 0.3, increasing with salinity (Fig. 4e).

The PARAFAC model identified three fluorescent components with CONCORDIA of 84.4%. Component 1 (C1) presented a fluorescence peak at an excitation/emission wavelength of 315 nm/420 nm. Coble (1996) defined this component (peak M) as a marine humic-like peak mainly derived from microbial-derived fulvic acids. However, component C1 is also like peaks found in terrestrial sources. Then, C1 corresponded to the mixture of humic compounds of marine and terrestrial origin (Stedmon and Markager 2005; Coble 2007). Component 2 (C2) was composed of two separate excitation peaks, the first (265 nm/465 nm) and the second (365 nm/465 nm), which were within the range for terrestrial humic compounds analyzed by Stedmon and Markager (2005) in estuarine waters. Component 3 (C3) was also composed of two separate excitation peaks, the first (285 nm/510 nm) and the second (405 nm/510 nm), that resembled a combination of humic-like fluorophores (A and C) derived from terrestrial source (Coble 2007) (Fig. 5).

These peaks were similar to fluorophores from estuarine environments (Parlanti et al. 2000; Stedmon and Markager 2005; Coble 2007). However, it was not possible to observe the differentiation between protein and humic-like DOM that occurs through emission wavelength, which is higher than 370 nm to humic-like DOM and lower than 370 nm to protein-like DOM.

Size distribution for organic matter and dissolved elements

The POC (> 0.7 µm) ranged from 10.9 to 31.8% of the total organic matter (TOM) in the Jaguaribe River estuary, and DOC ranged from 68.2 to 89.1% (Fig. 6a). The dominant fraction of DOC was < 1 kDa, the low molecular DOM (LMW-DOM) or truly dissolved organic matter (TDOM), ranging from 474.4 to 544.2 µmol L^{-1} (average of 505.9 ± 35.4 µmol L^{-1}). The LMW-DOM fraction corresponded to 63.5 to 82.6% of the TOM (Fig. 6a). The COM (0.7 µm > COM > 1 kDa) concentrations ranged of 25.8 to 39.3 µmol L^{-1}, with an average of 32.9 ± 4.9 µmol L^{-1}, that corresponded to 4.7 to 6.5% of the TOM (Fig. 6b).

Dissolved element concentrations are presented in Table 1. The order of average concentrations of them in the Jaguaribe River estuary was Sr > Al > Rb > Fe > Li > Mo > U > V > Cu > Ni > Pb > Cr > Sn. The elements were distributed mainly in the truly dissolved phase (< 1 kDa), as well as the DOM (Fig. 7a), corresponding to more than 90% of the bulk sample to each metal. The trace metals in the total colloidal phase (> 1 kDa) varied from 3.5 to 7.3% (Fig. 7 b–g).

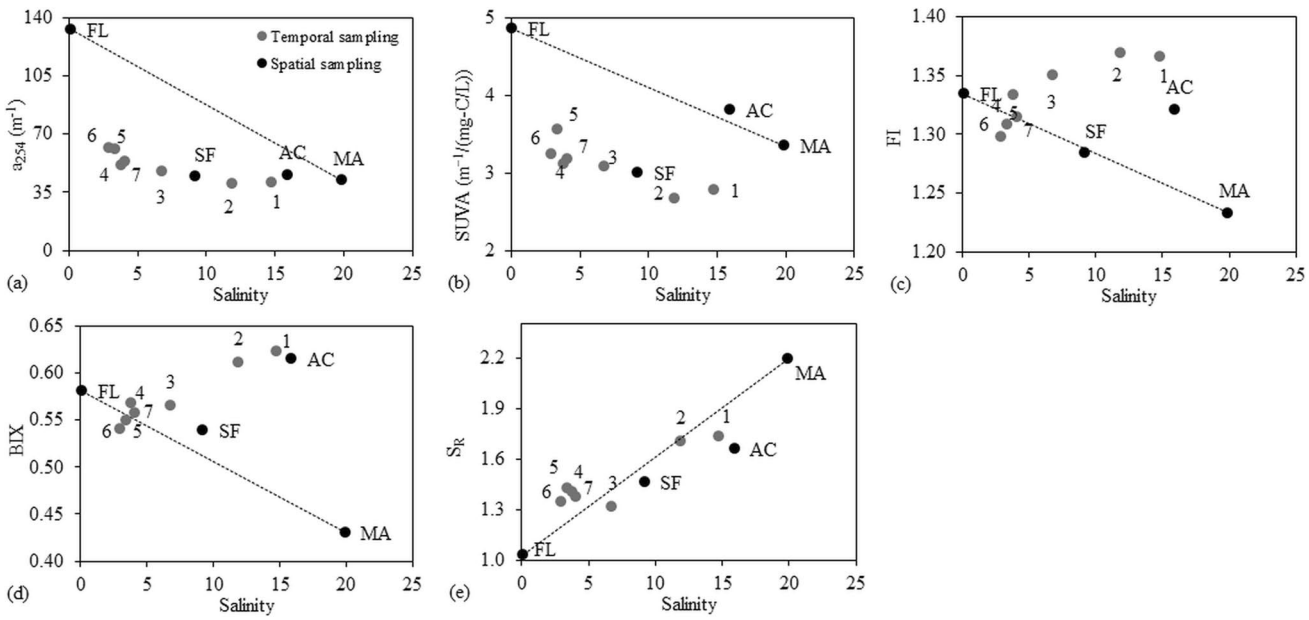

Fig. 4 Variation of the **a** a_{254} and **b** SUVA, **c** FI, **d** BIX, and **e** S_R with salinity. Numbers and letters refer to the samples from temporal and spatial sampling, respectively

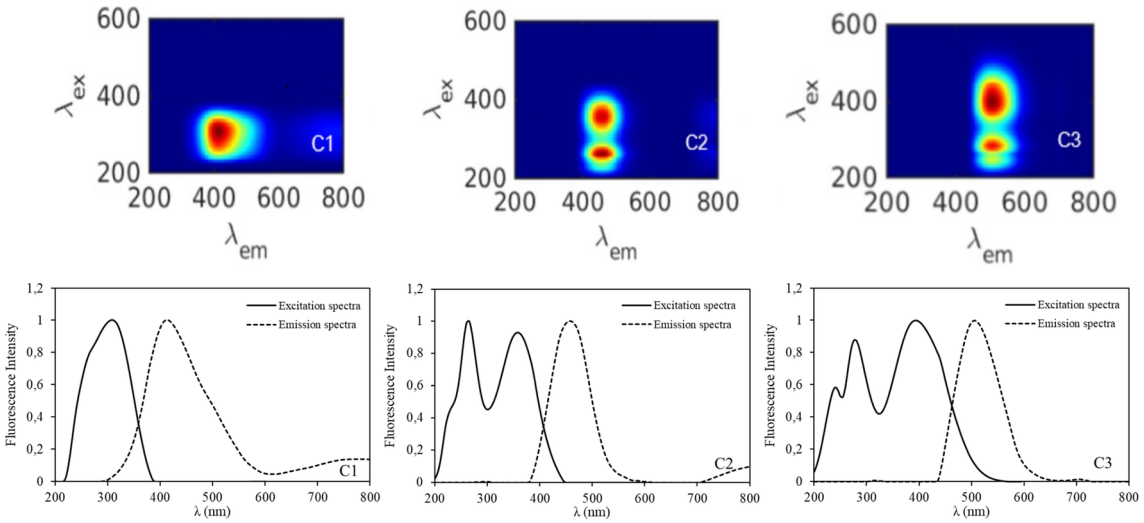

Fig. 5 Contour plots of three components (C1–C3) and the loadings of components of CDOM identified by the PARAFAC model. The solid and dotted lines represent the excitation and emission loadings, respectively

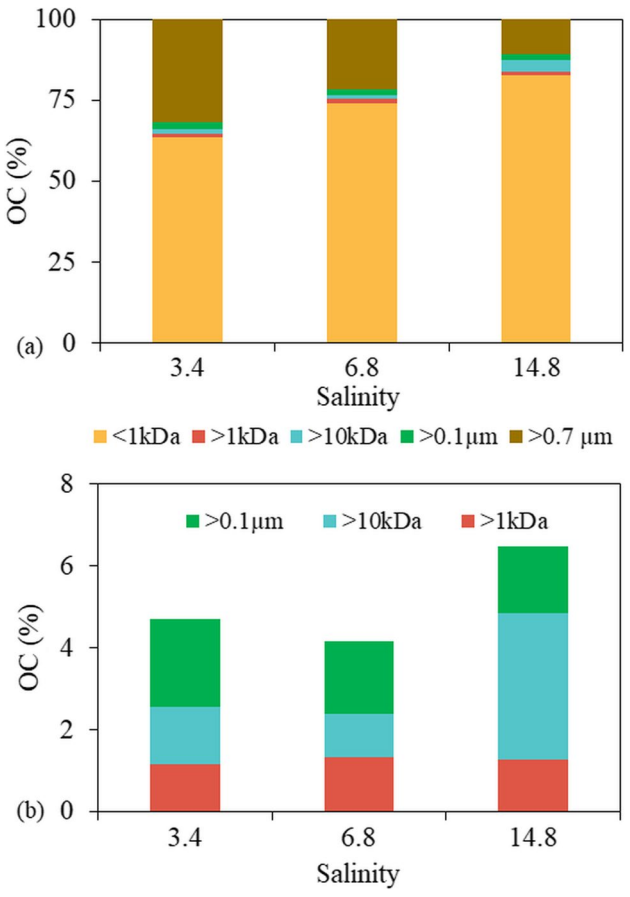

Fig. 6 Size distribution of **a** total and **b** colloidal organic carbon in the column water of the Jaguaribe River estuary with salinity variation

Table 1 Dissolved concentrations of elements in the bulk samples of the Jaguaribe River estuary and their correlation with DOC. Bold values are significant correlation at $p < 0.01$

Element	FL station (μg L^{-1})	MA station (μg L^{-1})	FP station, average ± STD (μg L^{-1})	Correlation with DOC
Li	1.81	73.99	26.16 ± 15.83	**−0.981**
Rb	3.20	95.39	30.17 ± 20.07	**−0.973**
Sr	176.10	5578.83	2270.71 ± 1469.49	**−0.973**
Mo	0.70	7.12	2.64 ± 1.09	**−0.982**
U	0.27	3.09	0.79 ± 0.37	**−0.964**
V	4.99	2.08	2.99 ± 0.47	**0.764**
Cr	0.92	0.06	0.09 ± 0.03	**0.854**
Fe	410.97	0.68	3.13 ± 1.41	**0.809**
Ni	2.20	0.54	1.26 ± 0.26	**0.809**
Cu	2.91	0.40	1.33 ± 0.33	**0.773**
Al	805.54	0.97	2.67 ± 1.36	**0.764**

Discussion

Behavior and temporal variation of the organic matter in the Jaguaribe river estuary

POC concentrations in this study were similar to those from September 2004 and 50% higher than in December 2016 (Table 2). Although previous data on POC are limited to dry seasons, its large variability probably shows that other drivers can contribute to the OC concentrations and partitioning besides rain-dependent natural processes, such as effluent emissions and upstream reservoirs' management (Marins et al. 2011; Dias et al. 2016; Mounier

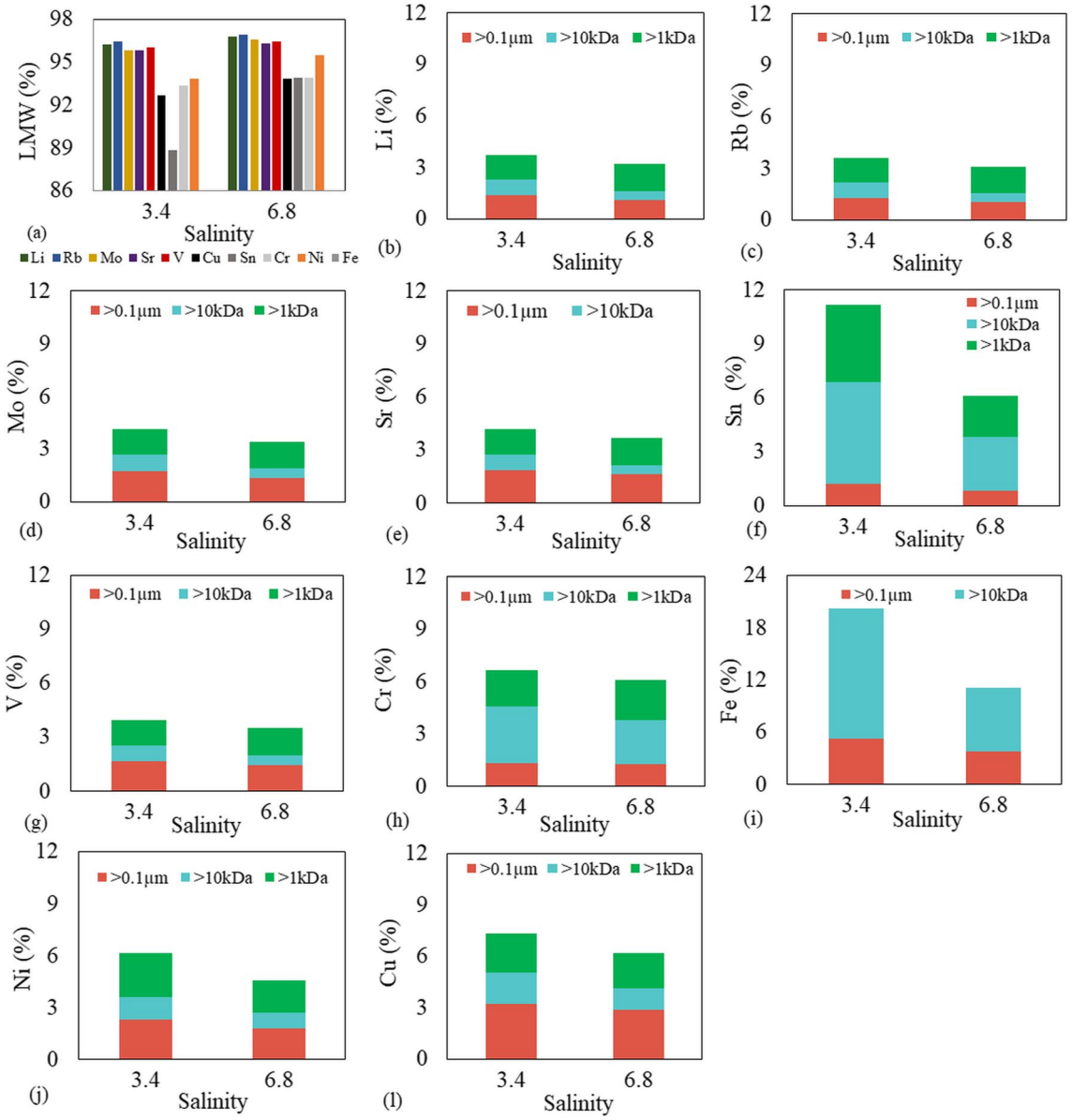

Fig. 7 **a** Distribution of the truly dissolved elements and colloidal size distribution of **b** Li, **c** Rb, **d** Sr, **e** Mo, **f** V, and **g** Cu with salinity variation in the Jaguaribe River estuary

Table 2 DOC and POC concentrations in the Jaguaribe River estuary (*campaigns performed in rainy season)

Sampling period	*n*	POC	DOC	Reference
May 2014*	13	-	419.1 ± 96.6	Cavalcante et al. (2021)
March 2016*	10	-	291.1 ± 159.2	Cavalcante (2019)
December 2016	10	61.0 ± 68.6	275.1 ± 162.3	Cavalcante (2019)
April 2004*	9	-	875 ± 491	Mounier et al. (2018)
September 2004	15	182.1 ± 48.3	1,200 ± 770.5	Mounier et al. (2018)
April 2018*	11	180.4 ± 88.5	597.0 ± 149.1	This study

et al. 2018; Cotovicz et al. 2022). The POC increase from salinity 0 to 5 indicates the existence of other relevant POC sources in the estuarine maximum turbidity zone besides those from the upstream. These sources are probably from the shrimp farm activity and sediments delivered from the impacted mangrove due to their proximity to the

FP station. Furthermore, the highest POC value occurred during the low tide when Cumbe channel input is highest.

Besides, the flocculation of DOM is an important salt-induced process in the estuarine maximum turbidity zone (Asmala et al. 2014). At low salinity, the decrease of DOC probably fed the POC pool until the sinking process occurred, then led to a loss for both POC and DOC. The inverse correlation between pH and DOC ($r = -0.733$; $p < 0.05$) indicated DOC removal through flocculation due to the increase of cationic strength (Zhu et al. 2014). The non-conservative behavior of POC and DOC showed complex organic matter processing in the Jaguaribe River estuary. Then, POC and DOC were not controlled only by marine dilution but also by biogeochemical processes, such as precipitation, adsorption/desorption, and microbial and photodegradation (Moyer et al. 2015).

The POC:Chl-*a* ratio was used to discriminate newly produced phytoplankton in POC (POC:Chl-*a* < 200 g g^{-1}) from detrital or degraded material (POC:Chl-*a* > 200 g g^{-1}) (Bianchi et al., 1997; Savoye et al., 2012, 2003). The POC:Chl-*a* ratio varied from 96.3 to 346.9, with an average of 161.1 ± 84.0, indicating that autochthonous sources were important to the OM bulk in the estuary, mainly in the highest salinity (Fig. 8). Besides, POC correlated positively with Chl-*a* ($r = 0.667$; $p < 0.05$). The POC:Chl-*a* ratio was lower in SF than in the AC and even at the MA, pointing out that the POC from Cumbe Creek is more labile than that from AC and the marine end-member (MA). The contribution of continental sources to the AC station was similar to the FL station, even its proximity to the sea, due to the influence of the mangrove forest (Cavalcante et al. 2021).

DOC concentrations decreased in the Jaguaribe River estuary due to the riverine discharge reduction caused by the 2012–2017 drought and river damming (Cavalcante et al. 2021; Mounier et al. 2018). In this study, DOC values were also lower (30%) than in April 2004 (Table 2) but around

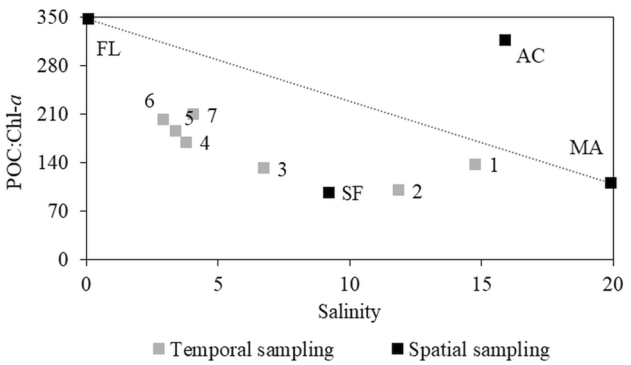

Fig. 8 POC:Chl-*a* ratio plotted against salinity. The conservative mixing line was calculated from fluvial and marine end-members. Numbers and letters refer to the samples from temporal and spatial sampling, respectively

50% higher than those measured by Cavalcante et al. (2019, 2021), probably due to the weakening of the drought in the region in 2018. Regarding the estimate for rivers in South America (Dai et al. 2012), the DOC concentration in Jaguaribe River was higher. Then, these results showed the effect of drought over organic matter input in the estuary and its large temporal variability, highlighting the importance of increasing data availability in semiarid ecosystems.

The Piauí River and the Salt River estuary are located in NE Brazil. They are under a similar climate to the Jaguaribe River estuary. Among them, the Salt River estuary is the one that suffers most from anthropogenic pressures, receiving industrial and domestic effluents and disposal of aquaculture activities. The Jaguaribe River estuary had DOC values similar to the Piauí River estuary (530.4 ± 152.1 µmol L^{-1}), which receives wastewater discharges from domestic sources and industries in its upper region (Costa et al. 2011). Compared with the Salt River estuary (DOC = 833.4 ± 78.6 µmol L^{-1}), the DOC average was lower in the Jaguaribe River estuary. However, at the river end-member (FL station), specifically, the values were similar (Arguelho et al. 2017). Then, DOC concentrations in the Jaguaribe River showed the contribution of anthropogenic sources and the OM sink during the estuarine mixing.

Riverine discharge is one of the principal controllers of phytoplankton biomass by nutrient availability and salinity changes (Oliveira et al. 2023). In this study, the increase in rainfall resulted in less saline and OM-enriched waters which might have enhanced phytoplankton growth (around three times) compared to the drought period (Cavalcante et al. 2021). However, the excessive increase of primary production can lead to a deterioration of water quality by eutrophication which is a worldwide pollution issue with harmful consequences as hypoxia, death of organisms, release of toxic gases or unpleasant odors, toxic algal blooms, and loss of biotic diversity (Nie et al. 2016). The response to environmental variation is site-specific, being necessary to understand well the system functioning for the better management and sustainable use of this ecosystem, mainly in regions strongly affected by climate changes (Cotovicz et al. 2022).

Optical properties of DOM

The strong relationship between DOC and CDOM ($r = 0.948$, $p < 0.01$) showed that CDOM is a representative fraction of the DOM in the Jaguaribe River estuary (Wang et al. 2004). More CDOM in freshwater than in estuarine water means that fluvial DOM is more subject to photodegradation because it is more susceptive to the absorption of light (Yi et al. 2014). Then, the photooxidation of DOM is intensified when fluvial DOM achieves less turbid waters in the estuary. $SUVA_{254}$ values above 3 m^{-1}/(mg-C/L) indicate

a high degree of aromaticity and unsaturation of the DOM that reflect environments with high terrestrial inputs. While lower values indicate low aromaticity and higher relative abundances of autochthonous DOM, being 1.8 m^{-1}/(mg-C/L) described as algae and bacterial-derived OM (Rosario-Ortiz et al. 2007) and 0.6 m^{-1}/(mg-C/L) as ocean samples (Weishaar et al. 2003). Most samples presented $SUVA_{254}$ values greater than 3, indicating that DOM was predominantly from terrigenous sources, different from POC. The high $SUVA_{254}$ value measured at the AC station compared to those in the estuary probably happened due to the contribution of the mangrove forest to the OM from this channel in the ebb tide, as observed by POC as well.

FI and BIX have been used to distinguish DOM derived from autochthonous (microbially and algal-derived DOM with FI > 1.9 and 0.8 < BIX < 1) from allochthonous sources (terrestrially-derived DOM with FI < 1.4 and BIX < 0.6) (Couturier et al. 2016; Yan et al. 2021). The Jaguaribe River estuary presented low BIX (0.54 ± 0.05) and FI (1.31 ± 0.04) values which showed the large contribution of terrestrial-derived humic-like DOM. In the fixed point, FI and BIX increased with salinity displaying a slight increase in autochthone production (Fig. 4c and d). Surprisingly, FI and BIX were lower in the marine than in the fluvial end-member, probably due to the release of OM from sediment resuspension caused by the tide at the downstream region (Krishna et al., 2015).

S_R values below 1 indicate terrestrial DOM with higher MW and aromaticity and above 1 indicates DOM with lower MW and more photodegraded DOM (Couturier et al. 2016). Higher S_R value is normally found in coastal waters than in freshwater due to the less aromatic DOM and more intense photobleaching process (Marcinek et al. 2020; Cao and Tzortziou 2024). Besides, it is also associated with the dominance of autochthone sources in marine waters (Yan et al. 2021). In the Jaguaribe River estuary, S_R values (1.4 ± 0.3) pointed to DOM with low MW and extensively degraded DOM. The positive relationship between S_R and salinity (Fig. 4e) suggested a decrease in the average molecular mass and aromatic content of CDOM with marine influence (Marcinek et al. 2020; Yan et al. 2021). As the BIX index was low, the contribution of biological compounds might have a minor relevance on S_R variation compared to the photodegradation and flocculation process.

Generally, CDOM and $SUVA_{254}$ decrease with salinity in estuaries. Some of them present conservative behavior related to the dilution by marine waters (Wang et al. 2014). While others show a non-conservative behavior caused by photodegradation, flocculation, and/or precipitation (Guo et al. 2007; Yamashita et al. 2010; Dixon et al. 2014). The non-conservative decrease of CDOM and $SUVA_{254}$ (Fig. 4a and b) indicated that the DOM suffered changes with the tide dynamics and through processes such as photooxidation and flocculation to the DOM (Dixon et al. 2014).

The three components were present along all the estuaries and showed the highest concentrations in the freshwater (Fig. 9a, b, and c). Their fluorescence intensity decreased non-conservatively with the increase of salinity. This behavior was similar to the terrestrial-derived OM components (peaks II, III, and IV) from the Piauí River estuary and the opposite to the fluorophore marine-derived (peak I) that increased with salinity (Costa et al. 2011). The fluorescence

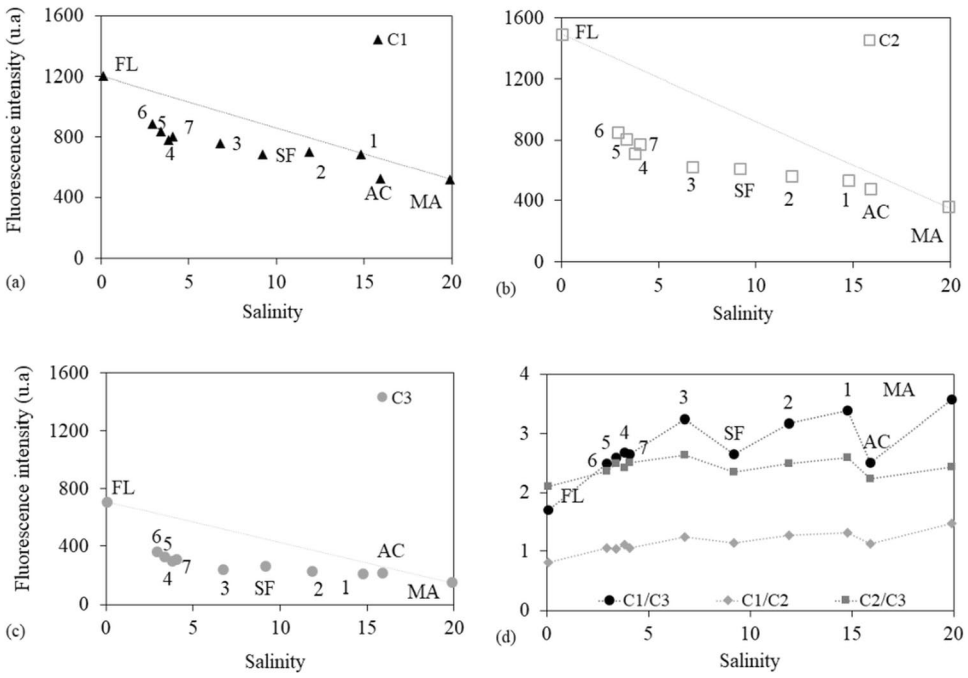

Fig. 9 Fluorescence intensity variation of **a** C1, **b** C2, **c** C3, and **d** components ratios with salinity. Numbers and letters refer to the samples from temporal and spatial sampling, respectively

intensity of terrestrial OM normally decreases with estuarine mixing as a result of the dilution, photobleaching, adsorption, and flocculation process (Guo et al. 2012; Osburn et al. 2012; Wang et al. 2014, 2017; Yi et al. 2014) as seen in the Jaguaribe river estuary. Then, the fluorescence and $SUVA_{254}$ results confirm the dominance of the terrestrial origin of the OM in the Jaguaribe River estuary during the rainy season.

Although the three components showed similar behavior, the relative contribution of each one indicates a change in the quality of the OM with the estuarine mixture (Fig. 9d). C2 was the component with the highest fluorescence intensity in the fluvial end-member, but the increase of C1/C2 ratio downstream showed a decrease of C2 contribution in relation to C1 (Fig. 9d). Besides, the ratio C1/C3 doubled with the salinity increase, while the C2/C3 was practically constant. The change in the proportion between the components along the salinity gradient occurred because the C1 is also composed of marine DOM, which increases with sea influence. The increase of C1 could also be a result of microbial degradation of fulvic acids in the estuarine zone. The loss of fluorescence is concomitant with DOC loss until a salinity of 7. Besides, a break occurs at this salinity for C1/C2 and C1/C3, meaning that the terrestrial organic matter preferentially settles from the dissolved to the particulate phase in low salinity levels.

Size distributions of OM with estuarine mixing

The fractionation of DOM in the Jaguaribe River estuary was similar to the Jiulong River Estuary, with DOM being preponderantly in the LMW fraction and derived from soil leaching (Yi et al. 2014). Mangroves might have been important contributors to the estuarine DOM in the Jaguaribe River, considering that the highest DOC concentrations were observed at low tide (Fig. 3b), when the DOM contribution derived from the mangrove through tidal pumping is higher (Bouillon et al., 2007; Rezende et al., 2007). Xu and Guo (2017) observed that DOM was mostly distributed within the LMW range, regardless of sample types (lake, river, and sea), and they suggested that DOM size was dependent of source and environmental conditions. However, the percentage of COM in the Jaguaribe River estuary was much lower than observed worldwide (Duan and Bianchi 2006; Guo et al. 2009; Stephens and Minor 2010; Xu and Guo 2017).

The concomitant reduction in POC and augmentation in LMW-DOM (Fig. 6a) indicate a diminution of OM size along the salinity gradient. Xu and Guo (2017) also observed an increase of LMW-DOM percentage from riverine to marine samples and they suggested a strict relation between particle size and their sources. Environmental settings can also cause particle size reduction during the physical mixing by processes such as photochemical and microbial degradation, disaggregation, and repartitioning. The disaggregation process converts organic aggregates into smaller size fractions as a consequence of the ionic strength increase (Xu et al. 2018). Another relevant process is the photodegradation, that reduces particle size and CDOM concentrations (Guo et al. 2012; Xu et al. 2018). The optical properties of the DOM and its size variation suggest photodegradation is an important driver in the OM cycling in the Jaguaribe River estuary.

The sum of the COM fractions presented an increasing tendency with salinity, but a reduction (~ 27%) was observed in an intermediary salinity 6.8 (Fig. 6b), reflecting the behavior of the DOM in bulk samples. Besides the conversion of COM in LMW with the salinity increasing, as mentioned above, the COM removal at salinity 6.8 might have been strengthened by flocculation that is commonly reported to a salinity level below 10 (Coble 2007).

Dissolved elements

The similarities among the dissolved metals were evaluated using multivariate cluster analysis (Online Resource 2). Two groups were clearly recognized. Group 1 comprising Cr, Fe, V, Al, Cu, Ni, Pb, and Sn and Group 2 including Li, Rb, Sr, Mo, and U. Group 1 clustered the variables with a non-conservative decline with salinity (Online Resource 3). The subgroups reflected their mobility since Cr, Fe, and V are classified as metals with low mobility, Ni and Cu as moderate lability, and the Al is among the most immobile elements (Gaillardet et al. 2013). The clustering of Li, Rb, Sr, Mo, and U was expected because they present conservative mixing behavior with salinity (Online Resource 3), indicating that sampling and analyses were well performed. Besides, they belong to the trace metal groups with high and moderated mobility (Gaillardet et al. 2013). Then these metals are found in high concentrations in seawater (Bruland and Lohan 2003).

Some metals of this group 1 (Cu, Ni, Fe, V, and Cr) presented a significant positive correlation with DOC (Table 2), being regulated by the DOM in the estuary. The DOM composition, predominantly of humic substances, has a strong complexing capacity with metals (Fang et al. 2015; Yang and Van Den Berg 2009). However, this interaction is worrying, because while DOM-metal association can stabilize toxic metals through their precipitation to bottom sediments, it can also make the contaminants available to the biota (Machado et al. 2016).

Some metals (e.g., Cu, Pb, and Cd) are normally associated with colloids in estuarine environments (Waeles et al. 2008), and their partitioning depends on the competition between ligands with high and low molecular weight. However, in the Jaguaribe River estuary, the metals were distributed mainly in the truly dissolved phase. The low concentration of metals in the colloidal phase might have occurred

due to the low concentration of COM in the Jaguaribe River estuary. Li, Rb, Sr, and Mo colloidal fractions were practically constant with salinity. However, the percentage of colloidal Cu, Fe, and Ni decreases at salinity 6.8 (Fig. 7f, g), as observed for the COM, being probably removed from column water by flocculation or repartitioning. DOM and trace metals were preponderantly in the truly dissolved fraction, suggesting their high mobility in the Jaguaribe River estuary. Besides, the OM modification along the salinity gradient might intensify its interaction with dissolved metals in the estuary. Then, this study contributed to the comprehension of the fate and behavior of contaminants in the Jaguaribe River estuary which are relevant information to evaluate and monitor the water quality depend on the organic matter association.

Conclusion

This study evaluated the sources and behavior of OM and dissolved metals in a semiarid estuary in NE Brazil, which has suffered from decreasing annual rainfall and freshwater inputs due to climate change and river damming. Besides, the estuary has been experiencing an increase of discharges from shrimp farm activity. The results showed the relevance of semiarid estuaries for better understanding the effects of global climate change and anthropogenic pressures over the carbon cycle. The variability of DOC concentrations in the Jaguaribe River estuary was shown to be a response to climate variability and anthropogenic pressures, suggesting that climatic change may influence the biogeochemistry of OM in this estuary.

Optical characteristics (FDOM, SUVA, BIX, and CDOM) and size distribution of the DOM showed the dominance of terrestrial/allochthone sources to the estuarine DOM, with a high aromaticity degree and associated with humic substances. However, the non-conservative behavior of DOM, CDOM, SUVA, FI, S_R, and FDOM indicated that the DOM was very reactive; it was removed from the column water during the estuarine mixing by processes such as flocculation, aggregation, and microbial and photodegradation. As the estuary is heterotrophic, it is possible that the signal of the protein-like FDOM (autochthone) has not been detected due to its rapid consumption by biological activity.

On the other hand, the POC:Chl-*a* ratio showed that POM was predominantly composed of phytoplankton. Besides, other sources (mangrove and shrimp farm) were relevant beyond of the fluvial and marine to the POM in the Jaguaribe River estuary. POM also presented a non-conservative behavior, being removed from column water in salinity above 4. The different sources of POC and DOC and their non-conservative behavior pointed out the complexity of the OM dynamic in the Jaguaribe River estuary. Future works must focus on understanding the DOM sink in the Jaguaribe River estuary because of its relevance in a global climatic change context, since photo or microbial degradation of the DOM enhances the increase of the CO_2 partial pressure, for example.

DOM was mostly distributed within the LMW fraction and presented a low percentage in the colloidal fraction, pointing to the great contribution of soil leaching and low production of autochthone DOM in the Jaguaribe River estuary, respectively. Dissolved metals presented the same size distribution than the DOM. Some elements (Li, Rb, Sr, Mo, and U) presented conservative behavior, being controlled by the mixing process, while others (Cu, Fe, Cr, and V) had non-conservative behavior with a significant positive correlation with DOM. The relationship of DOM with Cu and Cr is very worrying due to the high toxicity of these elements to the organisms.

Acknowledgements We acknowledge the support from the PRONEX/FUNCAP/CNPq Proc. No. PR2-0101- 29 00052.01.00/15 coordinated by Marins, RV who received a productivity scholarship from CNPQ No. 309718/2016-3.

We thank RSA Chielle, VL Moura, and ML Massari, members of the Coastal Biogeochemistry Laboratory (UFC/LABOMAR), for helping with the sampling. We thank the Mediterranean Institute of Oceanography laboratory, at Université de Toulon, for their support in the sample analysis.

Author contribution MS Cavalcante and RV Marins designed the study. MS Cavalcante and S Mounier conducted the analysis. MS Cavalcante, RV Marins, and S Mounier wrote the manuscript. All authors contributed to interpreting the results, discussions, writing, and refinement of the paper.

Funding Cavalcante, MS was funded by the PELD (Long-term Ecological Research Program) Brazilian Semiarid Coast (FUNCAP/CNPq 442337/2020–5) as part of the Brazilian LTER Program.

Data availability Data will be made available on request.

Declarations

Ethics approval We approve that this manuscript is part of the thesis of the author Cavalcante, MS (Cavalcante, 2019).

Consent for publication We give consent to publish a part of the PhD studies and is jointly contributed by all authors.

Conflict of interest The authors declare no competing interests.

References

Arguelho M de LP de M, Alves J do PH, Monteiro ASC, Garcia CAB (2017) Characterization of dissolved organic matter in an urbanized estuary located in Northeastern Brazil. Environ Monit Assess 189–272. https://doi.org/10.1007/s10661-017-5966-7

Asmala E, Bowers DG, Autio R et al (2014) Qualitative changes of riverine dissolved organic matter at low salinities due to

flocculation. J Geophys Res Biogeosci 119:1919–1933. https://doi.org/10.1002/2014JG002722
Bruland KW, Lohan MC (2003) Controls of trace metals in seawater. In: Holland HD, Turekian KK (eds) Treatise on geochemistry. Elsevier, pp 23–47
Cao F, Tzortziou M (2024) Impacts of hydrology and extreme events on dissolved organic carbon dynamics in a heavily urbanized estuary and its major tributaries: a view from space. J Geophys Res Biogeosci 129:1–23. https://doi.org/10.1029/2023JG007767
Cavalcante MS, Marins RV, Dias FJ da S, Rezende CE de (2021) Assessment of carbon fluxes to coastal area during persistent drought conditions. Reg Stud Mar Sci 47:101934 https://doi.org/10.1016/j.rsma.2021.101934
Coble PG (2007) Marine optical biogeochemistry: the chemistry of ocean color. Chem Rev 107:402–418. https://doi.org/10.1021/cr050350+
Coble PG (1996) Characterization of marine and terrestrial DOM in seawater using excitation-emission matrix spectroscopy. Mar Chem 51:325–346
Cory RM, McKnight DM (2005) Fluorescence spectroscopy reveals ubiquitous presence of oxidized and reduced quinones in dissolved organic matter. Environ Sci Technol 39:8142–8149. https://doi.org/10.1021/es0506962
Costa AS, Passos EDA, Garcia CA, Alves JDPH (2011) A characterization of dissolved organic matter in the Piauí River Estuary, Northeast Brazil. J Braz Chem Soc 22:2139–2147. https://doi.org/10.1590/S0103-50532011001100017
Costa BGB, Lacerda LD (2014) Mercury (Hg) in fish consumed by the local population of the Jaguaribe River lower basin, Northeast Brazil. Environ Sci Pollut Res 21:13335–13341. https://doi.org/10.1007/s11356-014-3297-6
Costa BGB, Soares TM, Torres RF, Lacerda LD (2013) Mercury distribution in a mangrove tidal creek affected by intensive shrimp farming. Bull Environ Contam Toxicol 90:537–541. https://doi.org/10.1007/s00128-012-0957-4
Cotovicz LCJ, Marins RV, da Silva ARF (2022) Eutrophication amplifies the diel variability of carbonate chemistry in an equatorial, semi-arid, and negative estuary. Front Mar Sci 9:1–18. https://doi.org/10.3389/fmars.2022.767632
Couturier M, Nozais C, Chaillou G (2016) Microtidal subterranean estuaries as a source of fresh terrestrial dissolved organic matter to the coastal ocean. Mar Chem 186:46–57. https://doi.org/10.1016/j.marchem.2016.08.001
Dai M, Yin Z, Meng F et al (2012) Spatial distribution of riverine DOC inputs to the ocean: an updated global synthesis. Curr Opin Environ Sustain 4:170–178. https://doi.org/10.1016/j.cosust.2012.03.003
Dantas JC, Silva RM, Santos CAG (2020) Drought impacts, social organization, and public policies in northeastern Brazil: a case study of the upper Paraíba River basin. Environ Monit Assess 192. https://doi.org/10.1007/s10661-020-8219-0
Dias FJ da S, Lacerda LD, Marins RV, de Paula FCF (2011) Comparative analysis of rating curve and ADP estimates of instantaneous water discharge through estuaries in two contrasting Brazilian rivers. Hydrol Process 25:2188–2201. https://doi.org/10.1002/hyp.7972
Dias FJ da S, Marins RV, Maia LP (2013) Impact of drainage basin changes on suspended matter and particulate copper and zinc discharges to the ocean from the Jaguaribe River in the semiarid NE brazilian coast. J Coast Res 29:1137–1145. https://doi.org/10.2112/JCOASTRES-D-12-00115.1
Dias FJDS, Castro BM, Lacerda LD et al (2016) Physical characteristics and discharges of suspended particulate matter at the continent-ocean interface in an estuary located in a semiarid region in northeastern Brazil. Estuar Coast Shelf Sci 180:258–274. https://doi.org/10.1016/j.ecss.2016.08.006
Dixon JL, Helms JR, Kieber RJ, Avery GB (2014) Biogeochemical alteration of dissolved organic material in the Cape Fear River Estuary as a function of freshwater discharge. Estuar Coast Shelf Sci 149:273–282. https://doi.org/10.1016/j.ecss.2014.08.026
Duan S, Bianchi TS (2006) Seasonal changes in the abundance and composition of plant pigments in particulate organic carbon in the lower Mississippi and Pearl Rivers. Estuaries Coasts 29:427–442. https://doi.org/10.1007/BF02784991
Eschrique SA, Braga EDS, Marins RV, Gonsalez V (2010) Nutrients as indicators of environmental changes in two Brazilian estuarine systems. Safety, Heal Environ World Congr 71–75
Fang K, Yuan D, Zhang L et al (2015) Effect of environmental factors on the complexation of iron and humic acid. J Environ Sci (china) 27:188–196. https://doi.org/10.1016/j.jes.2014.06.039
Fellman JB, Hood E, D'Amore DV et al (2009) Seasonal changes in the chemical quality and biodegradability of dissolved organic matter exported from soils to streams in coastal temperate rainforest watersheds. Biogeochemistry 95:277–293. https://doi.org/10.1007/s10533-009-9336-6
Findlay SEG, Sinsabaugh RL (2003) Aquatic ecosystems. Academic Press, San Diego
Gaillardet J, Viers J, Dupré B (2013) Trace elements in river waters
Giani M, Savelli F, Berto D et al (2005) Temporal dynamics of dissolved and particulate organic carbon in the northern Adriatic Sea in relation to the mucilage events. Sci Total Environ 353:126–138. https://doi.org/10.1016/j.scitotenv.2005.09.062
Godoy MDP, de Lacerda LD (2014) River-island morphological response to basin land-use change within the Jaguaribe River Estuary, NE Brazil. J Coast Res 294:399–410. https://doi.org/10.2112/jcoastres-d-13-00059.1
Godoy MDP, de Lacerda LD (2015) Mangroves response to climate change: a review of recent findings on mangrove extension and distribution. Ann Brazilian Acad Sci 87:651–667. https://doi.org/10.1590/0001-3765201520150055
Guo L, White DM, Xu C, Santschi PH (2009) Chemical and isotopic composition of high-molecular-weight dissolved organic matter from the Mississippi River plume. Mar Chem 114:63–71. https://doi.org/10.1016/j.marchem.2009.04.002
Guo W, Stedmon CA, Han Y et al (2007) The conservative and non-conservative behavior of chromophoric dissolved organic matter in Chinese estuarine waters. Mar Chem 107:357–366. https://doi.org/10.1016/j.marchem.2007.03.006
Guo W, Yang L, Yu X et al (2012) Photo-production of dissolved inorganic carbon from dissolved organic matter in contrasting coastal waters in the southwestern Taiwan Strait, China. J Environ Sci (china) 24:1181–1188. https://doi.org/10.1016/S1001-0742(11)60921-2
Gustafsson JP (2019) Vanadium geochemistry in the biogeosphere –speciation, solid-solution interactions, and ecotoxicity. Appl Geochem 102:1–25. https://doi.org/10.1016/j.apgeochem.2018.12.027
ISO (1992) Water quality measurement of biochemical parameters spectrophotometric determination of chlorophyll-a concentration. International Organization for Standardization, Geneva
Lacerda LD de, Marins RV, Dias FJ da S (2020) An arctic paradox: response of fluvial Hg inputs and bioavailability to global climate change in an extreme coastal environment. Front Earth Sci 8. https://doi.org/10.3389/feart.2020.00093
Lacerda LD, Dias FJS, Marins RV et al (2013) Pluriannual watershed discharges of Hg into a tropical semi-arid estuary of the Jaguaribe River, NE Brazil. J Braz Chem Soc 24:1719–1731. https://doi.org/10.5935/0103-5053.20130216
Lacerda LD, Molisani MM, Sena D, Maia LP (2008) Estimating the importance of natural and anthropogenic sources on N and P emission to estuaries along the Ceará State Coast NE Brazil.

Environ Monit Assess 141:149–164. https://doi.org/10.1007/s10661-007-9884-y
Lacerda LD, Santos JA, Madrid RM (2006) Copper emission factors from intensive shrimp aquaculture. Mar Pollut Bull 52:1823–1826. https://doi.org/10.1016/j.marpolbul.2006.09.012
Lacerda LD, Soares TM, Costa BGB, Godoy MDP (2011) Mercury emission factors from intensive shrimp aquaculture and their relative importance to the Jaguaribe River Estuary, NE Brazil. Bull Environ Contam Toxicol 87:657–661. https://doi.org/10.1007/s00128-011-0399-4
Lin H, Cai Y, Sun X et al (2016) Sources and mixing behavior of chromophoric dissolved organic matter in the Taiwan Strait. Mar Chem 187:43–56. https://doi.org/10.1016/j.marchem.2016.11.001
Louis Y, Garnier C, Lenoble V et al (2009) Characterisation and modelling of marine dissolved organic matter interactions with major and trace cations. Mar Environ Res 67:100–107. https://doi.org/10.1016/j.marenvres.2008.12.002
Luan H, Vadas TM (2015) Size characterization of dissolved metals and organic matter in source waters to streams in developed landscapes. Environ Pollut 197:76–83. https://doi.org/10.1016/j.envpol.2014.12.004
Machado AA de S, Spencer K, Kloas W et al (2016) Metal fate and effects in estuaries: a review and conceptual model for better understanding of toxicity. Sci Total Environ 541:268–281. https://doi.org/10.1016/j.scitotenv.2015.09.045
Marcinek S, Santinelli C, Cindrić AM et al (2020) Dissolved organic matter dynamics in the pristine Krka River estuary (Croatia). Mar Chem 225. https://doi.org/10.1016/j.marchem.2020.103848
Marengo JA, Alves LM, Alvala RC, et al (2017) Climatic characteristics of the 2010–2016 drought in the semiarid Northeast Brazil region. An Acad Bras Cienc 1–13. https://doi.org/10.1590/0001-3765201720170206
Marengo JA, Cunha APMA, Nobre CA et al (2020) Assessing drought in the drylands of northeast Brazil under regional warming exceeding 4 °C. Nat Hazards 103:2589–2611. https://doi.org/10.1007/s11069-020-04097-3
Marins RV, De LLD, Abreu IM, Dias FJDS (2003) Efeitos da açudagem no rio Jaguaribe. Ciência Hoje 33:66–70
Marins RV, Paula Filho FJ, Eschrique SA, Lacerda LD (2011) Anthropogenic sources and distribution of phosphorus in sediments from the Jaguaribe River estuary, NE, Brazil. Brazilian J Biol 71:673–678. https://doi.org/10.1590/S1519-69842011000400011
Mounier S, Marins RV, Lacerda LD de (2018) Characterization of the Ceara costal zone organic matter inputs. Archives-Ouverts 39
Moura VL, de Lacerda LD (2018) Contrasting mercury bioavailability in the marine and fluvial dominated areas of the Jaguaribe River Basin, Ceará, Brazil. Bull Environ Contam Toxicol 101:49–54. https://doi.org/10.1007/s00128-018-2368-7
Moyer RP, Powell CE, Gordon DJ et al (2015) Abundance, distribution, and fluxes of dissolved organic carbon (DOC) in four small subtropical rivers of the Tampa Bay Estuary (Florida, USA). Appl Geochem 63:550–562. https://doi.org/10.1016/j.apgeochem.2015.05.004
Nie Z, Wu X, Huang H et al (2016) Tracking fluorescent dissolved organic matter in multistage rivers using EEM-PARAFAC analysis: implications of the secondary tributary remediation for watershed management. Environ Sci Pollut Res 23:8756–8769. https://doi.org/10.1007/s11356-016-6110-x
Oliveira ARG, Queiroz JBM, Pardal EC et al (2023) How does the phytoplankton community respond to the effects of La Niña and post-drought events in a tide-dominated Amazon estuary? Aquat Sci 85:1–23. https://doi.org/10.1007/s00027-022-00904-0
Osburn CL, Handsel LT, Mikan MP et al (2012) Fluorescence tracking of dissolved and particulate organic matter quality in a river-dominated estuary. Environ Sci Technol 46:8628–8636. https://doi.org/10.1021/es3007723
Parlanti E, Wörz K, Geoffroy L, Lamotte M (2000) Dissolved organic matter fluorescence spectroscopy as a tool to estimate biological activity in a coastal zone submitted to anthropogenic inputs. Org Geochem 31:1765–1781. https://doi.org/10.1016/S0146-6380(00)00124-8
Rios JHL, Marins RV, Oliveira KF, Lacerda LD (2016) Long-Term (2002–2015) Changes in mercury contamination in NE Brazil depicted by the mangrove oyster Crassostraea rhizophorae (Guilding, 1828). Bull Environ Contam Toxicol 97:474–479. https://doi.org/10.1007/s00128-016-1855-y
Rosario-Ortiz FL, Snyder SA, Suffet IH, (Mel. (2007) Characterization of dissolved organic matter in drinking water sources impacted by multiple tributaries. Water Res 41:4115–4128. https://doi.org/10.1016/j.watres.2007.05.045
Santinelli C, Nannicini L, Seritti A (2010) DOC dynamics in the meso and bathypelagic layers of the Mediterranean Sea. Deep Res Part II Top Stud Oceanogr 57:1446–1459. https://doi.org/10.1016/j.dsr2.2010.02.014
Shin Y, Lee E-J, Jeon Y-J et al (2016) Hydrological changes of DOM composition and biodegradability of rivers in temperate monsoon climates. J Hydrol 540:538–548. https://doi.org/10.1016/j.jhydrol.2016.06.004
Simpson SL, Vardanega CR, Jarolimek C et al (2014) Metal speciation and potential bioavailability changes during discharge and neutralisation of acidic drainage water. Chemosphere 103:172–180. https://doi.org/10.1016/j.chemosphere.2013.11.059
Soares MO, Campos CC, Carneiro PBM et al (2021) Challenges and perspectives for the Brazilian semi-arid coast under global environmental changes. Perspect Ecol Conserv 19:267–278
Stedmon CA, Bro R (2008) Characterizing dissolved organic matter fluorescence with parallel factor analysis: a tutorial. Limnol Oceanogr Methods 6:572–579. https://doi.org/10.4319/lom.2008.6.572b
Stedmon CA, Markager S (2005) Resolving the variability in dissolved organic matter fluorescence in a temperate estuary and its catchment using PARAFAC analysis. LimnolOceanogr 50:686–697
Stedmon CA, Markager S, Kaas H (2000) Optical properties and signatures of chromophoric dissolved organic matter (CDOM) in Danish coastal waters. Estuar Coast Shelf Sci 51:267–278. https://doi.org/10.1006/ecss.2000.0645
Stephens BM, Minor EC (2010) DOM characteristics along the continuum from river to receiving basin: a comparison of freshwater and saline transects. Aquat Sci 72:403–417. https://doi.org/10.1007/s00027-010-0144-9
Stolpe B, Guo L, Shiller AM, Hassellöv M (2010) Size and composition of colloidal organic matter and trace elements in the Mississippi River, Pearl River and the northern Gulf of Mexico, as characterized by flow field-flow fractionation. Mar Chem 118:119–128. https://doi.org/10.1016/j.marchem.2009.11.007
Stolpe B, Zhou Z, Guo L, Shiller AM (2014) Colloidal size distribution of humic- and protein-like fluorescent organic matter in the northern Gulf of Mexico. Mar Chem 164:25–37. https://doi.org/10.1016/j.marchem.2014.05.007
Tribovillard N, Algeo TJ, Lyons T, Riboulleau A (2006) Trace metals as paleoredox and paleoproductivity proxies: an update. Chem Geol 232:12–32. https://doi.org/10.1016/j.chemgeo.2006.02.012
Waeles M, Tanguy V, Lespes G, Riso RD (2008) Behaviour of colloidal trace metals (Cu, Pb and Cd) in estuarine waters: an approach using frontal ultrafiltration (UF) and stripping chronopotentiometric methods (SCP). Estuar Coast Shelf Sci 80:538–544. https://doi.org/10.1016/j.ecss.2008.09.010
Wang W, Chen M, Guo L, Wang WX (2017) Size partitioning and mixing behavior of trace metals and dissolved organic matter in a South China estuary. Sci Total Environ 603–604:434–444. https://doi.org/10.1016/j.scitotenv.2017.06.121

Wang XC, Altabet MA, Callahan J, Chen RF (2004) Stable carbon and nitrogen isotopic compositions of high molecular weight dissolved organic matter from four U.S. estuaries. Geochim Cosmochim Acta 68:2681–2691. https://doi.org/10.1016/j.gca.2004.01.004

Wang Y, Zhang D, Shen Z et al (2014) Characterization and spacial distribution variability of chromophoric dissolved organic matter (CDOM) in the Yangtze Estuary. Chemosphere 95:353–362. https://doi.org/10.1016/j.chemosphere.2013.09.044

Wang Y, Zhang D, Shen Z, yao, et al (2015) Investigation of the interaction between As and Sb species and dissolved organic matter in the Yangtze Estuary, China, using excitation–emission matrices with parallel factor analysis. Environ Sci Pollut Res 22:1819–1830. https://doi.org/10.1007/s11356-014-3380-z

Wang Z gang, Liu W qing, Zhao N jing, et al (2007) Composition analysis of colored dissolved organic matter in Taihu Lake based on three dimension excitation-emission fluorescence matrix and PARAFAC model, and the potential application in water quality monitoring. J Environ Sci 19:787–791. https://doi.org/10.1016/S1001-0742(07)60132-6

Weishaar JL, Aiken GR, Bergamaschi BA et al (2003) Evaluation of specific ultraviolet absorbance as an indicator of the chemical composition and reactivity of dissolved organic carbon. Environ Sci Technol 37:4702–4708. https://doi.org/10.1021/es030360x

Wilkinson KJ, Lead JR (2007) Environmental colloids and particles: behaviour, separation and characterisation BT - IUPAC series on analytical and physical chemistry of environmental systems v. 10

Xu H, Guo L (2017) Molecular size-dependent abundance and composition of dissolved organic matter in river, lake and sea waters. Water Res 117:115–126. https://doi.org/10.1016/j.watres.2017.04.006

Xu H, Houghton EM, Houghton CJ, Guo L (2018) Variations in size and composition of colloidal organic matter in a negative freshwater estuary. Sci Total Environ 615:931–941. https://doi.org/10.1016/j.scitotenv.2017.10.019

Yamashita Y, Maie N, Briceño H, Jaffé R (2010) Optical characterization of dissolved organic matter in tropical rivers of the Guayana Shield, Venezuela. J Geophys Res Biogeosciences 115:. https://doi.org/10.1029/2009JG000987

Yan L, Xie X, Peng K et al (2021) Sources and compositional characterization of chromophoric dissolved organic matter in a Hainan tropical mangrove-estuary. J Hydrol 600:126572. https://doi.org/10.1016/j.jhydrol.2021.126572

Yang L, Chen CTA, Lui HK et al (2016) Effects of microbial transformation on dissolved organic matter in the east Taiwan Strait and implications for carbon and nutrient cycling. Estuar Coast Shelf Sci 180:59–68. https://doi.org/10.1016/j.ecss.2016.06.021

Yang R, Van Den Berg CMG (2009) Metal complexation by humic substances in seawater. Environ Sci Technol 43:7192–7197. https://doi.org/10.1021/es900173w

Yi Y, Zheng A, Guo W et al (2014) Optical properties of estuarine dissolved organic matter isolated using cross-flow ultrafiltration. Acta Oceanol Sin 33:22–29. https://doi.org/10.1007/s13131-014-0451-4

Zepp RG, Sheldon WM, Moran MA (2004) Dissolved organic fluorophores in southeastern US coastal waters: correction method for eliminating Rayleigh and Raman scattering peaks in excitation-emission matrices. Mar Chem 89:15–36. https://doi.org/10.1016/j.marchem.2004.02.006

Zhou Z, Guo L (2015) A critical evaluation of an asymmetrical flow field-flow fractionation system for colloidal size characterization of natural organic matter. J Chromatogr A 1399:53–64. https://doi.org/10.1016/j.chroma.2015.04.035

Zhu G, Yin J, Zhang P et al (2014) DOM removal by flocculation process: fluorescence excitation-emission matrix spectroscopy (EEMs) characterization. Desalination 346:38–45. https://doi.org/10.1016/j.desal.2014.04.031